A Dynamical Model to study the Response of Microalgae to Pulse Amplitude Modulated Fluorometry

F. Chazalon*, S. Rabouille*, P. Hartmann*, A. Sciandra*, O. Bernard*,**

** LOV, UMR 7093, B.P. 28, 06234 Villefranche-sur-mer, France*
*** BIOCORE, INRIA, B.P. 93, 06902 Sophia-Antipolis Cedex, France*

Abstract: On-line monitoring growth of microalgal based processes is a challenging issue. Pulse Amplitude Modulated (PAM) fluorometers, used to closely monitor the physiological state of photosystems, do not provide an estimation of the growth rate, a critical information for culture management. We designed a model to represent the relation between the fast dynamics of photosynthesis and the slower process of cell growth in microalgae as a function of light. This model provides a synthetic view of photosystem II photochemistry and accounts for the main two states (open and closed) of photosystem II reaction centres as well as the following electron transport chain. The model is used to analyse the link between a very fast process (the transition between closed and open states), an intermediate one (the filling of the quinone-plastoquinone pool) and a slow process (growth rate fluctuations). Experiments were conducted on the Haptophyceae *Tisochrysis lutea*. Model parameters were calibrated on the measured fluorescence data. A slow-fast analysis is presented to describe the system dynamics. Results provide new insights for understanding and interpreting PAM measurements.

1. INTRODUCTION

Microalgae are microscopic photosynthetic organism with increasing biotechnological applications (Mata et al. 2011). Their composition offers very diverse high value compounds in the fields of pharmaceutics, cosmetics or food, as well as the potential production of biofuel (Chisti, 2007). Yet so far, phototrophic microorganisms have been less exploited than bacteria or yeast, mostly because their growth- which is directly driven by photosynthesis-- strongly depends on environmental conditions.

On-line monitoring of microalgal-based bioprocesses is thus a crucial challenge (Bernard, 2011; Mairet et al. 2012). Although quite accurate, deriving the growth rate from cell counts or dry biomass weight measurements is costly, time consuming, and not immediate. Comparatively, real-time photosynthetic activity can be obtained by measuring microalgae fluorescence with a non-invasive, sensitive and fast method (Govindjee, 1995). Unfortunately, the rate of photosynthesis is not a direct, experimental proxy of the growth rate. Better comprehension of these two processes can be expected by a modelling analysis at the time scale of the photosystem dynamics.

Photosynthesis initiates in photosystems (PS), the elementary bricks of the photosynthetic apparatus, in which photons are converted into chemical energy. This process is very fast, typically in the order of milliseconds. Photons absorbed by the photosystem antenna turn it into an excited state. Three distinct paths of de-excitation are possible to bring the reaction centre back to the ground state: (i) re-emission of a photon (fluorescence); (ii) initiation of photosynthesis through a series of photochemical reactions involving electrons transport in the cell membrane, called photochemical quenching (Maxwell and Johnson, 2000); (iii) non-photochemical quenching through, e.g., thermal dissipation. The term "quenching" refers to any process lowering fluorescence (Krause et Weis, 1991). Pulse Amplitude Modulated (PAM) fluorometers (Quick and Horton, 1984; Schreiber, 1986) excite photosystems and measure the resultant fluorescence. Two kinds of photosystems are present on cells: type I (PSI) and type II (PSII). Fluorescence emission from PSI is independent from the state of the reaction centre (Butler, 1978), so that fluorescence variations can be attributed to PSII alone. We will work under this hypothesis, and the model we will derive will represent the state of PSII.

The goal of the present study is to use a model in order to gain more information from PAM measurements. The model represents the excitation of PSII centres in response to light and their consequent fluorescence dynamics. In particular, the model is used to analyze the links between a very fast process (the PSII photosynthetic yield) and a slow one (the cell growth rate). Experimental data, acquired on cultures of *Tisochrysis lutea* growing exponentially, are used for model calibration. Qualitative and quantitative analyses of the model are then performed.

2. PAM OPERATION

During the photochemical quenching process, chlorophyll *a* molecules transfer their excitation to the reaction centre P_{680} (RC2) of PSII. A succession of oxidation-reduction steps reduces the first quinone Q_A (figure 1) and the photosystem closes: energy can no more be transferred to RC2 until Q_A is reoxidized by the downstream electrons acceptors Q_B and PQ. The corresponding energy transfer through the electron transport chain eventually leads to CO_2 fixation.

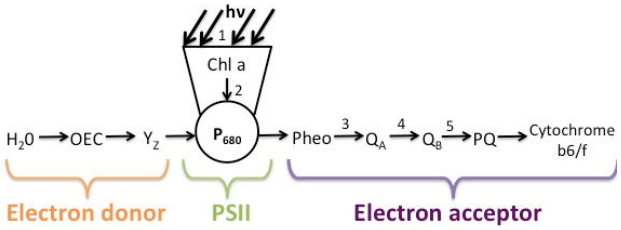

Fig. 1. Decomposition of the photochemical reaction steps. Chl a: chlorophyll a; P_{680}: reaction centre, Pheo: Pheophytin molecule; Q_A and Q_B: quinones A and B; PQ: plastoquinone; Y_z: a tyrosine molecule; OEC: Oxygen Evolving Complex; P: PSII; D and A: electron donors and acceptors.

The irradiance applied to the microalgae in a PAM results from the sum of three elementary light signals: (i) a constant, background irradiance at a chosen intensity to create an ambient light field which will partly close the reaction centres; (ii) brief saturating pulses whose very high intensity closes all reaction centres and (iii) a pulsed, light with very weak intensity (typically, lower than 1 $\mu E.m^{-2}.s^{-1}$). All three induce fluorescence, but while the first two are said "actinic" as they trigger photosynthesis, the third one is the measuring light, whose crenel shape allows for the detection of fluorescence capacity variations in the PAM by signal filtering.

3. MATERIAL AND METHODS

3.1. Species considered

The unicellular photosynthetic eukaryote *Tisochrysis lutea* (Bendif *et al.* 2013) was used for the experiments. Cultures were grown at 27°C under a light intensity of 400 $\mu E.m^{-2}.s^{-1}$. Fluorescence monitoring was performed on subsamples from the cultures taken in the exponential phase of growth.

3.2. Experimental procedures

Fluorescence measurements were conducted with a Multicolor PAM (Walz, Effeltrich, Germany) using a blue excitation light. Samples were diluted in filtered sea water and incubated in the dark for twenty minutes prior to measurement. The excitation protocol used is described in figure 2. Fluorescence is recorded for increasing levels of actinic light, and two saturating pulses are applied at each irradiance level.

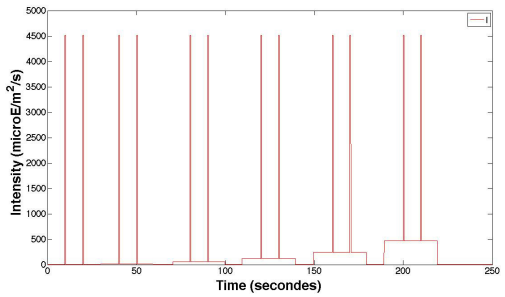

Fig. 2. Excitation protocol applied to the sample in order to calibrate the model.

4. MODEL DESIGN

4.1. The fluorescence model

After the reception of a photon, PSII undergoes several excitation phases depending on the oxidation (or reduction) state of the donor and acceptor molecules. In the present model, these phases are represented in a simplified manner by only two states: The fraction A, representing open photosystems, and the fraction B, representing the closed photosystems. Contrary to other existing models (Eilers and Peeters 1993, Han, 2002) we do not explicitly represent the dynamics of damaged and inhibited states of PSII following the reception of excess photons. However, due to the short time scales of measurements within a PAM (a few minutes), we will consider a dynamics of PSII deactivation due to light stress. The total number of non deactivated PSII is given by *n*, which decreases depending on the received light I:

$$\dot{n} = -\alpha_0 \cdot D \cdot n \qquad (1)$$

where D is the cumulative damage to the photosystem: $\dot{D} = I$. By abuse of notation, A will be called the proportion of open PSII (in the total number of non inhibited states), the total number of open PSII being nA. Closed PSII (of proportion B=1-A, and of number nB) are associated to various level of quinone and plastoquinone pool oxidation. Hence, we gathered quinones and plastoquinones in a pool receiving electrons from the B state, and the degree of reduction of this pool is denoted *q*. The pool is normalized, meaning that when q is 1, the maximum electron carrying capacity has been reached. The conceptual scheme is represented on figure 3.

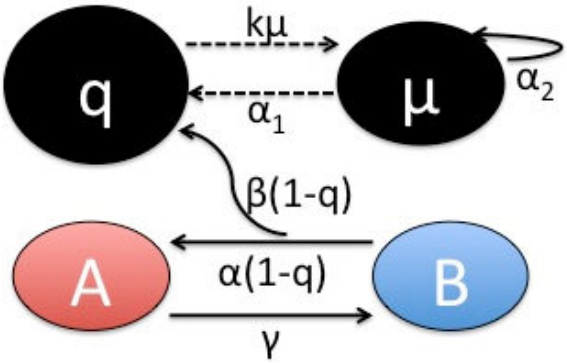

Fig. 3. Model conceptual scheme. Dashed and solid lines represent qualitative and quantitative relationships between variables, respectively

The photon flux closes reaction centres (transition from A to B) while their re-opening (transition from B to A) depends on the downstream flux of electrons through pool (q). Equation (2) expresses the dynamics of A:

$$\dot{A} = -\gamma(I) \cdot A + \alpha \cdot B \cdot (1-q) \qquad (2)$$

where α tunes the return from state B to A, this transfer being higher when electrons have been used and *q* is close to zero. The function γ controls the transfer rate from the state A to B. Since γ(I)/I is decreasing with I, we assume the following function:

$$\gamma(I) = \tilde{\gamma} \cdot I \frac{I + K_I}{I + \varepsilon}$$

in which ε, K_I and $\tilde{\gamma}$ are constants, with ε << K_I. The dynamics of the quinone/plastoquinone pool is then:

$$\dot{q} = \beta \cdot B \cdot (1 - q) - k\mu q \quad (3)$$

The term $\beta \cdot B \cdot (1-q)$ represents the rate of electrons filling pool q. The energy flux is mainly used in the Calvin cycle and leads to CO_2 fixation, i.e. biomass growth. The growth rate, denoted μ therefore modulates the rate at which electrons are consumed in chemical reactions. In our model, we assume that the fraction of light energy dissipated under non photochemical quenching (mainly heat) is constant.

Constant β controls the refill rate of quinone/plastoquinone, while the rate of electron use is associated to constant *k*. In order to represent the (slow) resulting changes in the growth rate, we introduced the following growth dynamics:

$$\dot{\mu} = \alpha_1 \cdot q - \alpha 2 \cdot \mu \quad (4)$$

Electrons departing from the pool q stimulate the growth rate.

Finally, the fluorescence for a given state (A,q) is the sum of a constant background fluorescence and a fluorescence due to the impossibility of state B to use the excess of photonic energy:

$$F = A_1 \cdot I \cdot n \cdot B + F_0 \cdot I$$

Where F_0 is the fluorescence obtained when photosystems are all open. Constant A_1 is the fluorescence rate per unit of actinic light.

4.2. *PAM measurements*

The PAM performs two fluorescence measurements: F^+ at the light I + δI and F^- at I (δI is the measurement light):

$$F^+ = A_1 \cdot (I + \delta I) \cdot B + F_0 \cdot (I + \delta I)$$

$$F^- = A_1 \cdot I \cdot B + F_0 \cdot I$$

Finally, the information which is given is

$$F_D = \frac{F^+ + F^-}{\delta I} = A_1 \cdot n \cdot B + F_0$$

For B = 1 (all reaction centres are closed), the PAM response is called F_m. And for B = 0 (all reaction centres are open), $F_D = F_0$.

Model equations, expressed with variable B=1-A, read:

$$\dot{B} = \gamma(I) \cdot (1 - B) - \alpha \cdot B \cdot (1 - q)$$

$$\dot{q} = \beta \cdot B \cdot (1 - q) - k\mu q$$

$$\dot{\mu} = \alpha_1 \cdot q - \alpha_2 \cdot \mu$$

$$\dot{D} = I$$

$$\dot{n} = -\alpha_3 \cdot D \cdot n$$

5. DYNAMICS ANALYSIS

5.1. Quantitative analysis of the model for a constant growth rate

We studied the model dynamic behaviour in the case of a constant μ. This simplification is reasonable as both B and q vary much faster than μ. The nullcline for q is given by:

$$B^* = \frac{k \cdot \mu \cdot q^*}{\beta(1 - q^*)} \quad (a)$$

The nullcline for B is given by,

$$B^* = \frac{\gamma(I)}{\gamma(I) + \tilde{\alpha} - \tilde{\alpha} \cdot q^*} \quad (b)$$

Taking into account the expression of γ(I), it becomes:

$$B^* = \frac{I \cdot \tilde{\gamma}(I + K_I)}{(I + \varepsilon) \cdot \left\{ I \cdot \tilde{\gamma} \cdot \frac{I + K_I}{I + \varepsilon} + \tilde{\alpha} - \tilde{\alpha} \cdot q^* \right\}} \quad (b)$$

The equilibrium results from the intersection of the two nullclines. This equilibrium is unique. Indeed, at the equilibrium point we get:

$$\frac{k \cdot \mu \cdot q^*}{\beta \cdot (1 - q^*)} = \frac{\gamma(I)}{\gamma(I) + \tilde{\alpha} - \tilde{\alpha} \cdot q^*}$$

Which gives π(q) = 0, with:

$$\pi(q) = -\tilde{\alpha} k \mu q^{*2} + [k\mu(\gamma(I) + \tilde{\alpha}) + \gamma(I)] q^* - \gamma(I)\beta$$

With the chosen parameters, and $\forall I \in [0.05, \quad 4516]$, the determinant Δ is strictly positive.

Moreover, It can be checked that:

$$\pi(1) = \gamma(I)(k\mu + 1 - \beta) > 0,$$

showing that 1 is between the two roots of the equation. Finally, since π(0) < 0, only one root is in the physical domain [0,1].

***Property**: the equilibrium (B*, q*,μ*) of the subsystem (B, q,μ) is globally asymptotically stable on the physical domain.*

Sketch of the proof: first note that variables B and q are both bounded between 0 and 1:

$\dot{B}|_{B=0} \geq 0$ and $\dot{B}|_{B=1} \leq 0$

$\dot{q}|_{q=0} \geq 0$ and $\dot{q}|_{q=1} \leq 0$

Variable μ is also lower bounded. Since q<1, we have

$\dot{\mu}|_{\mu=\alpha_1/\alpha_2} = \alpha_1 (q - 1) \leq 0$

The bounds of these variables define the (convex) physical domain.

Moreover, if we consider the change of variable ρ = 1-q, the system (B, ρ, q) is competitive in the sense that the extradiagonal terms of the Jacobian matrix are all non positive.

The computation of the Jacobian matrix at steady states shows that the equilibrium is locally stable.

As a consequence, for this three dimensional system, if there is a single locally stable equilibrium in the physical domain in which the system stays, this equilibrium is globally stable (Smith, 1995).

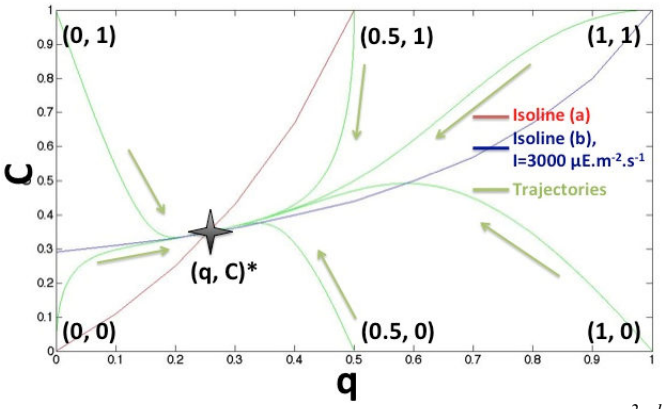

Fig. 4. Phase plane of the model for I = 100 µE.m^{-2}s^{-1} including the simulation of some trajectories starting from different initial points (C,q). The black cross represents the equilibrium point. Arrows show the direction of the model trajectories. Black numbers are the coordinates of the initial points and the equilibrium.

5.2. Simulation of the response to a flash in presence of actinic light: a slow fast analysis

Here we focus on the subsystem (B,q), assuming a constant growth rate (the dynamics of the growth rate is slower than that of B and q). We first show that it is a slow fast system of the type:

$$\theta \dot{B} = f(B, q)$$
$$\dot{q} = g(B, q)$$

With the parameter choice from Table 1, we get the following equations:

$$\dot{B} = \gamma I(1 - B) - 2B(1 - q)$$
$$\dot{q} = 0.2B(1 - q) - 0.4\mu q$$

For $I \geq 200$, $\theta = 0.1$ and there is a 10 times faster dynamics for C than for q.

The behaviour of the system can then be analysed as a response to the classical PAM measurement protocol. Dark-incubation is first performed to fully reduce (re-open) all reaction centres and let electrons drain away from pools, so that initially B=0 (all the reaction centres are open) and q=0 (no electron in the plastoquinone pool).

An example of dynamics following light stimulations is presented in figure 5. A sub-saturating actinic light of 200 µE.m^{-2}.s^{-1} is applied; the system (q, B) moves along path (1) and reaches the equilibrium corresponding to this new irradiance level. This is first done by rapidly reaching the slow manifold:

$$B(q) = \gamma(I)/(\gamma(I) + \alpha(1 - q))$$

The dynamics of the system then reduces to:

$$\dot{q} = \beta B(q)(1 - q) - k\mu q ,$$

Then q goes towards its equilibrium, continuously increasing. Since B(q) is an increasing function of q, during this period on the slow manifold, B is also increasing.

Then, a saturating flash is applied (2), B rapidly increases and reaches a new pseudo equilibrium so a new slow manifold value is reached for I=3000 µE.m^{-2}.s^{-1}. The new value obtained for B(q) is then very close to 1. Since the flash is brief, q hardly changes in the meantime. After the flash (3), B rapidly decreases to reach its new value B(q). Variable q still slowly increases towards its equilibrium (the plastoquinone pool is filling up). Finally, B and q decrease (4) until they reach back the equilibrium point corresponding to the constant, 200 µE.m^{-2}.s^{-1} ambient irradiance.

This slow-fast dynamics is characteristics of the measured response of fluorescence as a response to constant light – flash – constant light (figure 2).

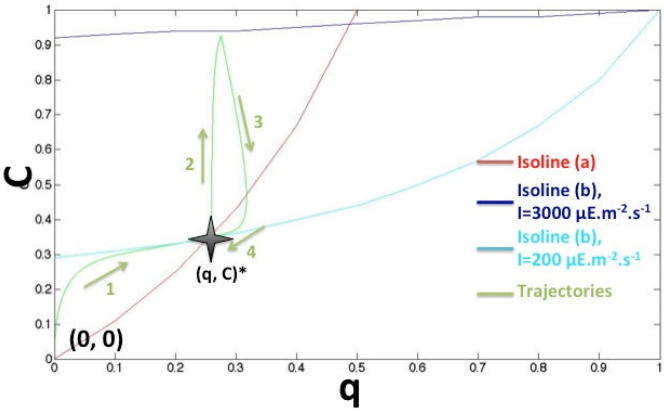

Fig. 5. Representation of variables trajectories during a flash, in presence of actinic light. The black cross represent the equilibrium point for I = 100 µE.m^{-2}.s^{-1}. Arrows show the direction of model trajectories. The successive steps are represented by green numbers.

5.3. Model calibration/parameter identification

Table 1. Parameter values

Parameter	Value	Units
β	0.2	s^{-1}
$\tilde{\gamma}$	0.007	$m^2.\mu E^{-1}$
k	0.4	s
α	2	s^{-1}
α_1	0.5	s^{-1}
α_2	0.005	-
α_3	$1.8*10^{-7}$	$m^2.\mu E^{-1}.s^{-1}$
A_1	0.4	-
K_I	200	$\mu E.m^{-2}.s^{-1}$
ε	80	$\mu E.m^{-2}.s^{-1}$
k	500	-
Chl	10^{15}	-

The model was calibrated using experimental data obtained in an experiment where multiple excitations have been made

(table 1). The results are then compared to new experimental data.

The experimental fluorescence and the fluorescence from the model simulation are compared on Figure 6. Two saturating pulses have been applied firstly in dark condition and then in the case of five increasing light levels. After each level of sub-saturating actinic light, the intensity of light comes back to 0.05 $\mu E.m^{-2}.s^{-1}$ (measuring light).
The maximum fluorescence level from the flashes diminishes through time in the case of both the simulation and the experiment. The levels of fluorescence decrease through time after the application of actinic sub-saturating light, especially in the case of the last levels of fluorescence.

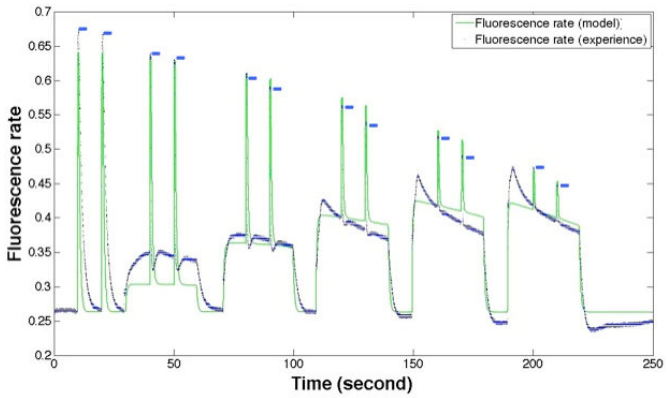

Fig. 6. Variation of experimental (blue curve) and simulated (green curve) fluorescences through time. Blue dashes locate the maximum of fluorescence in the experimental data.

6. DISCUSSION

The model describes experimental data with fair accuracy, and in particular the fluorescence levels following application of saturating pulses. The decrease in fluorescence after a flash is mainly due to the combination of both the natural decrease in B under lower light and the destruction of a fraction of reaction centres due to the succession of flashes of high intensity (dynamics of n). This could also be represented by a variation in the amount of energy dissipated through non photochemical quenching.
Fluorescence equilibria obtained for different sub-saturating, actinic light levels are relatively well described by the model. The slope of the simulated, last three levels are not as pronounced as in the experiment. The last levels of fluorescence resulting from the actinic sub-saturating light level showed a decrease through time. This could be explained by the progressive activation of carbon fixation processes (photochemical quenching). This may result from a change in the growth rate μ, which is poorly described by the model and which may lead to an increased demand in electrons, thus reducing more rapidly the fluorescence. This part of the model must probably be validated using microalgae sampled from cultures with different growth rates. Coherency between these growth rates and parameter μ in the model must be checked. The model could then be used to inverse the problem and estimate μ from the dynamics of fluorescence.

7. CONCLUSION

The present study proposed a synthetic view of the photosynthetic apparatus dynamics. The model involves three different scale of variation: a fast one for the direct response to the absorbed photons, an intermediate one for the filling of the quinone/plastoquinone pool and a slow one for the microalgal growth rate. The qualitative behaviour of the model was analysed and fairly matches the known response of fluorescence to a light pulse. The model has been calibrated based on PAM measurements on *Tisochrisis galbana*. More work remains to be done to better describe the dynamics of the growth rate μ.
The model will then be used to design an observer in order to estimate the growth rate μ from the measurements of the fluorescence response to series of flashes, and thus provide a simple way to monitor the status of a microalgal culture.

Acknowledgements: this work was supported by the ANR-13-BIME-004 Purple Sun.

REFERENCES

Bendif, E. M., Probert, I., Schroeder, D. C. and de Vargas, C. (2013). On the description of *Tisochrysis lutea* gen. nov. sp. nov. and *Isochrysis nuda* sp. nov. in the Isochrysidales, and the transfer of *Dicrateria* to the Prymnesiales (Haptophyta). Journal of Applied Phycology, **25**(6), 1763-1776.

Bernard, O. (2011). Hurdles and challenges for modelling and control of microalgae for CO_2 mitigation and biofuel production. Journal of Process Control, 21(10), 1378-1389.

Butler W.L. (1978). Energy distribution in the photochemical apparatus of photosynthesis. *Ann. Rev. Plant. Physiol.,* **29**, 345–378.

Chisti, Y. (2007). Biodiesel from microalgae. *Biotechnology advances*, **25(3)**, 294-306.

Eilers, P. H. C. and Peeters, J. C. H. (1993). Dynamic behaviour of a model for photosynthesis and photoinhibition. Ecological modelling, 69(1), 113-133.

Govindjee, R. (1995). Sixty-three years since Kautsky: Chlorophyll a fluorescence. *Australian Journal of Plant Physiology*, **22**, 131-160.

Han, B. P. (2002). A mechanistic model of algal photoinhibition induced by photodamage to photosystem-II. Journal of theoretical biology, 214(4), 519-527.

Krause, G.H., Weis, E. (1991). Chlorophyll fluorescence and photosynthesis: the basics. *Annual review of plant biology*, **42(1)**, 313-349.

Mairet, F., and Bernard, O. (2009). Coupling framers to get enhanced interval observers. Application to growth rate estimation in a photobioreactor. In the

proceedings of the 48th IEEE CDC/CCC 2009 conference. pp. 7581-7586.

Mata, T.M., Martins, A.A. and Caetano, N.S. (2010). Microalgae for biodiesel production and other applications: A review. *Renewable and Sustainable Energy Reviews*, **14(1)**, 217-232.

Maxwell, K., Johnson, G.N. (2000). Chlorophyll fluorescence – a practival guide. *Journal of Experimental Botany*, **51(345)**, 659-668.

Quick, W.P., Horton, P. (1984). Studies of the induction of chlorophyll fluorescence in Barley protoplast. I. Factors affecting the observation of oscillations in the yield of chlorophyll fluorescence and the rate of oxygen evolution. *Proceedings of the Royal Society of London*, Series B, **220**, 361-370.

Schreiber, U. (2004). Pulse-amplitude-modulation (PAM) fluorometry and saturation pulse method: an overview. In: *Chlorophyll a Fluorescence*. (Papageorgiou, G.C., Govindjee, R. (Ed)). 279-319. Springer. Netherlands.

Schatz, G. H., Brock, H., Holzwarth, A. R. (1988). Kinetic and energetic model for the primary processes in photosystem II. *Biophysical journal*, **54(3)**, 397-405.

Smith, H. L. (1995). Monotone Dynamical Systems, Vol. 41. *Mathematical Surveys and Monographs*.